

**Enhancement of skin efficacy and barrier function by skin lipid enhancer incorporated-lipid nanoparticles through the interaction with *stratum corneum***

Jihyun Lee, Minjoo Noh, Jihui Jang, **Jun Bae Lee**\*  
Innovation Lab, Cosmax R&I, Korea

The corresponding author:

Jun Bae Lee

Inno valley E-401, 255 Pangyo-ro, Bundang-gu, Seongnam-si, Gyeonggi-do, Korea

+82 31 789 3192

[jblee@cosmax.com](mailto:jblee@cosmax.com)

### **Abstract (Maximum of 250 words)**

In this work, we investigated the skin efficacy of skin lipid enhancer incorporated lipid nanoparticles (SLE-LNPs). Ceramide and fatty acids were used as SLE to improve the dermal delivery of cosmetic formulations. The measurements of particle size distribution and zeta potential of lipid nanoparticles (LNPs) with or without SLE have shown the effect of fatty acids to emulsion stability for 4 weeks. The morphology and structure have been investigated using SAXS and TEM. We demonstrate by both *in vitro* and *in vivo* skin penetration studies that SLE-LNPs including both ceramide and fatty acids show much improved penetration depth and faster rate compared to ordinary lipid nanoparticles (LNPs) without SLE as well as LNPs with only ceramide. In addition, as a result of *in vivo* clinical trials, SLE-LNPs has a statistically significant wrinkle decrease rate and melanin index decrease rate compared to the control group, resulting in a better skin efficacy effect. This results might indicate that SLE-LNPs can effectively interact with the SC, resulting in efficient skin delivery of the active agents such as niacinamide and adenosine, resulting improve skin efficacy. This strategy of incorporating both ceramide and fatty acids in LNPs provides a simple and easy route for the rapid and effective delivery of active ingredients across the skin barrier layer.

**Keywords:** Skin lipid enhancers (SLE); Lipid nanoparticles (LNP); Dermal delivery; Skin efficacy; Fatty acid

## **Introduction**

Dermal delivery of cosmetic formulations has been widely investigated for years. Recently, our cosmetic industry has prioritized how to improve the skin permeation of active agents and boost skin efficacy such as decreasing wrinkles and brightening the skin. There are three main permeation routes of cosmetic formulations across *stratum corneum* (SC); intercellular, intracellular and follicular pathways [1]. The SC intercellular lipids mainly contain ceramides, cholesterol, free fatty acids, etc [2]. Because the intercellular pathway through the intercellular lipids predominates over the intracellular and follicular pathways, development of cosmetic formulations using intercellular skin lipid composition might be useful approach to enhance skin permeation. The lateral packing order of skin lipids is also important for determining the permeability of the skin. There are three types of packing arrangements in intercellular spaces: the fluid lamellar phase, which is highly disordered and highly permeable, the hexagonal packing order of medium permeability, and the orthorhombic packing order exhibiting less permeability and a highly ordered state [3,4].

Ceramide, consists of fatty acid amide bound to a sphingoid base, is well known as an essential material for skin barrier functions. This is the reason why ceramides are constantly consumed and studied by people despite their limitations of crystallization. However, the importance of fatty acids capable of playing important roles in biological process such as normal structure and permeability barrier function of the SC are relatively rarely examined. In respects of skin penetration, free fatty acids, such as oleic acid (OA) can partition into lipid membranes and alter their physicochemical properties [5]. Golden et al. and Takeuchi et al. demonstrated that *cis*-unsaturated OA may fluidize SC lipid and thereby enhance membrane [6,7].

Herein, we aimed to utilize ceramide and fatty acid as SLE, which increase lateral diffusivity and fluidity of the SC lipid and interact with keratin [8]. We prepared SLE-LNPs composed of lipid matrix such as lecithin, ceramide, cholesterol derivatives, and fatty acids. The effect of fatty acid on colloidal stability was investigated by measuring the particle size distribution and zeta potential, and the morphology and structure were analyzed by measuring SAXS and Cryo-TEM. In this work, we investigate the skin effects such as skin penetration and skin efficacy of cosmetic formulations consisting of SLE-LNPs. Thus, our work would be helpful

for the understanding of skin penetration mechanism and skin efficacy by improved skin permeation.

## Materials and Methods

### Materials

Ceramide-NP (Doosan, Korea), hydrogenated lecithin (Lipoid GmbH, Switzerland), choleth-24 (polyethylene glycol ether of cholesterol with an average ethoxylation value of 24, Nihon Emulsion, Japan), dipropylene glycol (DPG), butylene glycol (BG), niacinamide (LASONS, India) and arbutin (HANGZHOU LINGEBA TECHNOLOGY, China) were commercially obtained. Stearic acid, oleic acid, FITC(Fluorescein-5-isothiocyanate), Sodium dodecyl sulfate (SDS), Trypsin-EDTA were purchased from Sigma Aldrich (USA). Two types of reconstructed human skin equivalent model, EpiDerm<sup>TM</sup> and EpiTEM<sup>TM</sup> were each purchased from MatTek Corporation (USA) and ROKIT HEALTHCARE INC (Korea), respectively. Reconstructed Human Pigmented Epidermis (SkinEthic<sup>TM</sup>) was purchased from Episkin Laboratories (France). All materials were of analytical grade. For all experiments, deionized double distilled water was used.

### Preparation of LNPs and SLE-LNPs with cosmetic active ingredients

The amounts of active agents such as niacinamide, adenosine, and arbutin was set to satisfy minimum amount notified by the Korean Ministry of Food and Drug Safety. Cosmetic formulations with ceramide, fatty acids, lecithin and choleth-24 were dissolved in DPG and BG at 90 °C while active ingredients and other additives were dissolved in distilled water at 80 °C. Then, DPG solution was slowly dropped to the water phase solution and the mixture was stirred with Agi-mixer to afford the skin carrier formulation. Here, the formulation that contains all the components is denoted as LNP-CF while the analogous one that excludes fatty acids is LNP-C and the one even without ceramide is referred as LNP. The detail of formulations including active ingredients are listed in **Table 1**.

**Table 1** Composition of LNP and SLE-LNP formulations containing active ingredients.

Ingredients	LNP	LNP-C	LNP-CF
Choleth-24	0.1	0.1	0.1
Lecithin	0.3	0.3	0.3
Ceramide-NP	-	0.05	0.05
Stearic acid	-	-	0.03
Oleic acid	-	-	0.03
Butylene glycol	5	5	5
Diropylene glycol	5	5	5
Niacinamide	2	2	2
Adenosine	0.04	0.04	0.04
Water	To 100	To 100	To 100
<sup>a</sup> Additives	q.s	q.s	q.s

<sup>a</sup>Additives are ethylenediaminetetraacetic acid (EDTA) and preservative.

### Physicochemical characterization of LNP and SLE-LNP formulations

The particle size and zeta potential of LNPs and SLE-LNPs were measured using dynamic light scattering (DLS, SZ-100, HORIBA, Japan). The excitation light source was a 10 mW He–Ne laser at 632.8 nm and the intensity of the scattered light was measured at 90°. All measurements were repeated three times and the average value was reported.

And, the morphology study of cosmetic formulations was performed by a cryogenic transmission electron microscopy (Tecnai F20 electron microscope, FEI, USA). Each sample was loaded onto Lacey Formvar / Carbon on 200 mesh Copper thick grid and immersed in liquid ethane to freeze them rapidly. The frozen samples were observed by cryo-TEM at an acceleration voltage of 200 kV.

The structure of formulations was characterized using small angle X-ray scattering (SAXS) analysis. The measurements was carried out using the 4C beamline of the Pohang Light Source II (PLS II) with 3 GeV power at the Pohang University of Science and Technology (Korea). A light source from an in-vacuum undulator 20 (IVU20: 1.4 m length, 20 mm period) of the Pohang Light Source II storage ring was focused with a vertical focusing toroidal mirror coated with rhodium and monochromatized with a Si (111) double crystal monochromator (DCM), yielding an X-ray beam wavelength of 0.734 Å. The X-ray beam

size at the sample stage was  $0.1\text{ (V)} \times 0.3\text{ (H) mm}^2$ . A two-dimensional (2D) charge-coupled detector (Mar USA, Inc.) was employed. The magnitude of the scattering vector,  $q = (4\pi/\lambda) \sin \theta$ , was  $0.02\text{ \AA}^{-1} < q < 0.25\text{ \AA}^{-1}$  for SAXS, where  $2\theta$  is the scattering angle and  $\lambda$  is the wavelength of the X-ray beam source. The scattering angle was calibrated with a silver behenate standard. A multi-sample stage was used, with a diameter of 4 mm and wall thickness of 1 mm, as bulk sample cells. All scattering measurements were carried out at room temperature. Each 2D pattern was radially averaged from the beam center and normalized to the transmitted X-ray beam intensity, which was monitored with a scintillation counter placed behind the sample. The scattering of distilled water was used as the experimental background.

### ***In vitro* skin penetration study**

To estimate the boosting effect of SLE in dermal delivery, *in vitro* Franz diffusion cell study was performed. Niacinamide (NA) was used as model drug and a synthetic membrane (Strat-MTM membrane (Transdermal diffusion test model, 25 mm), Merck, USA) were selected as model skin equivalent. Skin equivalent was fixed between the donor and the receptor chamber with the stratum corneum facing the donor compartment. The receptor compartment was filled with 7 mL of Phosphate Buffered Solution (pH 7.4), and has been maintained at  $32 \pm 0.5\text{ }^\circ\text{C}$  by circulating water by water jacket and continuously stirring at 350 rpm for 24 h. An aliquot (200  $\mu\text{L}$ ) of the samples was applied on the surface of the stratum corneum of the donor compartment. After 2, 4, 8, 24 hours of application of the formulations, the receptor phase (1 mL) was withdrawn through the sampling port of the receptor compartment, and the receptor compartment was refilled with the receptor phase to maintain a constant volume. The amount of NA that has permeated through the skin equivalent was analyzed by HPLC (Ultimate 3000, Dionex) with a reversed phase column (Jupiter® 5  $\mu\text{m}$  C18 300  $\text{\AA}$ , 250  $\times$  4.6 mm, Phenomenex). The mobile phase was 10 mM KH<sub>2</sub>PO<sub>4</sub>:Acetonitrile = 93:7 and the flow rate was 1 mL/min, and UV detection of the analyte was performed at 263 nm wavelength.

And, *in vitro* skin penetration study using fluorescent dyes was performed to visually investigate the effect of SLE in dermal delivery. The skin permeation of LNPs and SLE-LNPs through 3D artificial human skin equivalent (EpiDerm™(EPI-200), MatTek

Corporation, USA) was visualized with confocal laser scanning microscopy (CLSM). For fluorescence labelling of the cosmetic formulations, FITC (0.003 wt%) was added to the ones. Each fluorescently-labelled formulation (30 µL) was gently applied to the surface of 3D skin and the skin has been incubated for 8 hours at 37 °C, 5% CO<sub>2</sub> condition. After incubation for 8 h, the 3D skin was fixed with 3.7% formaldehyde solution for 1h and washed with PBS. After detaching the 3D skin sheets from the support membrane with Trypsin-EDTA, the sheets were frozen with embedding medium (O.C.T. compound) and sectioned at a thickness of 20 µm using a cryostat microtome (CM1850, Leica). After staining nucleus with DAPI, the stained 3D skin was visualized by CLSM at the Central Laboratory of KangWon National University (FV 1000 SPD, Olympus, Tokyo, Japan). FITC was excited with at 488 nm, DAPI was excited at 408 nm.

#### ***In vitro* skin brightening efficacy study**

Niacinamide is a brightening functional ingredient that inhibits hyperpigmentation by suppressing the transfer of melanin(melanosomes) from melanocytes to keratinocytes. The brightening efficacy of skin carrier containing niacinamide (NA) was performed using 3D reconstructed human pigmented epidermis (SkinEthic™-Brown (Phototype VI, EPISKIN, France). The 3D skin (0.63 cm<sup>2</sup> surface) composed of normal human-derived epidermal keratinocyte and melanocytes was pre-incubated in maintenance medium for 24 h at 37°C with 5% CO<sub>2</sub>. All media were replaced with fresh growth medium containing α-MSH to induce melanin formation by the melanocytes in the presence or absence of either lipid carrier (40 µL) containing niacinamide for 24 h. After incubation for 24 h, the skin tissue was fixed with 3.7% formaldehyde solution for 1h and washed with PBS. After detaching the 3D skin sheets for the support membrane with Trypsin-EDTA, the sheets embedded in paraffin blocks were sectioned at a thickness of 3 µm using a microtome (RM2235, Leica). To visualize the melanin distribution in the epidermis, the tissue sections were stained with a Fontana-Masson staining and to stain melanin and the cross-section of the tissue was observed using an optical microscope (BX53T, Olympus, Japan).

Arbutin also functions as a brightening agent that inhibits melanin synthesis by inhibiting tyrosinase. The overall experimental method is the same as described above, but the other details are mentioned. The 3D reconstructed human epidermis (SkinEthic™ - Brown

(Prototype VI, EPISKIN, France) was cultured with  $\alpha$ -MSH medium and exposed to each skin carrier (30  $\mu$ L) containing arbutin every 2 days for 8 days. The conditioned medium was replaced inside the insert every 2 days for 8 days. Phosphate buffered saline-treated skin well was used as negative controls. After incubation for 8 days, relative depigmentation was measured in the 3D skin model compared to after treatment with phosphate-buffered saline by L-values acquired using a spectrophotometer (KONICA Minolta, Tokyo, Japan). The images were obtained using an optical microscope (BX53T, Olympus, Japan).

### ***In vivo* skin penetration study**

*In vivo* human skin penetration study was carried out using confocal Raman spectroscopy (Skin composition analyzer<sup>®</sup> Model 3510 SCA, River Diagnostics, The Netherlands). Raman fingerprint spectra ( $400\text{-}1800\text{ cm}^{-1}$ ) were measured using 785 nm laser and the axial spatial resolution was 5  $\mu\text{m}$ , the spectral resolution was  $4\text{ cm}^{-1}$ . The integration time was 5 s for each depth. Raman fingerprint spectra were recorded starting from skin surface down to a depth of 24  $\mu\text{m}$ , in a step size of 2  $\mu\text{m}$ , at least 5 times.

Twenty healthy female subjects aged from 23 to 59 years old (average 44.1 years old) met the criteria for inclusion and none of the exclusion criteria participated in this study. The experiments were conducted by Skin Biotechnology Center of KyungHee University and approved by the Institutional Review Board (IRB) with IRB approval number: KHUSBC 2021-006R. All study participants signed a consent form before the start of the study and received information about the study procedures. Before the measurements, the subjects cleansed the test area of volar forearms and rested for 20 minutes under constant temperature and humidity (temperature  $22\pm2^\circ\text{C}$ , humidity  $50\pm10\%$ ) without air movement or direct sunlight.

After randomly setting the applied area ( $2 \times 3\text{ cm}^2$ ) of the two formulations among the left and right volar forearms, 200  $\mu\text{L}$  of each formulation was applied and sufficiently absorbed for 20 minutes, and gently wiped off with a tissue to remove any excess formulation from the surface of the skin. To evaluate the formulation permeation through the stratum corneum, the study was divided into three sets of measurements; Before application (Before); immediately after application (20 min, 20 minutes after application); after absorption (60 min, 60 minutes after application). The difference in penetration amount of the formulation before,

immediately after application (20 min), and 60 min after application, at each time point and the skin depth was statistically analyzed by using SPSS 26. According to the Skin Biotechnology Center's protocol (KHSP-002-V.1), the formulations are considered to have been penetrated, if the measured value has increased statistically significantly compared to before application, and discontinuous results at one stage of depth are interpreted as penetrated.

The data were analyzed using SkinTools v.2.0 (River Diagnostics, Rotterdam, The Netherlands) and statistical evaluation was performed using SPSS 26<sup>®</sup> (IBM SPSS Statistics, USA).

### ***In vivo* skin brightening study**

Subjects were selected as 22 adults aged 34 to 55 years (average  $44.2 \pm 6.42$  years old) who had hyperpigmentation sites and met the selection criteria. The clinical trial experiments were conducted by Clinical Research Associates Korea Incorporated (CRA Korea) and approved by the Institutional Review Board (IRB) with IRB approval number: 2020021201-202008-HR-003-01. Two formulations, LNP (control group) and LNP-CF (experimental group), were randomly assigned to both faces of the subject to be used twice a day for 4 weeks, respectively. The average usage per time was calculated by measuring the weight of the product at the start and end of the test and the number of uses recorded in the usage record. For the cheek, which is the measurement site, before, 2 weeks after use, and 4 weeks after use, skin melanin index measurement and photography were performed to conduct comparative evaluation of the product before and after use.

Melanin index, the absorptivity of the pigments at specific wavelengths, was measured with Mexameter<sup>®</sup> MX18 (MDD4, Courage+Khazaka electronic GmbH, Germany), defines the skin pigmentation related to melanin content in the skin. Measurements are performed by the application of a probe to the skin surface. The probe has a 5 mm aperture that emits 3 specific light wavelengths, green:  $\lambda = 568$  nm, red:  $\lambda = 660$  nm, and infrared:  $\lambda = 880$  nm. These radiations are reflected by the skin and captured back by the same probe. The results are expressed as an index value for each parameter in arbitrary units from 0 to 999, suggesting whitening improvement as the value decreases.

### ***In vivo* skin wrinkle study**

The clinical trial study for *in vivo* skin wrinkles improvement was conducted by Clinical Research Associates Korea Incorporated (CRA Korea Co., Ltd.) (IRB approval number: 2020021201-202008-HR-002-01), and the subject was selected as 20 adults aged 43 to 60 ( $52.5\pm5.12$  years old) with wrinkles around the eyes and a global photodamage score of 3 or more.

Two formulations, LNP (control group) and LNP-CF (experimental group), were randomly assigned to both faces of the subject to be used twice a day for 4 weeks, respectively. The average usage per time was calculated by measuring the weight of the product at the start and end of the test and the number of uses recorded in the usage record. For the eye area, which is the measurement site, before, 2 weeks after use, and 4 weeks after use, skin topography measurement and photography were performed to conduct comparative evaluation of the product before and after use. Skin topography was measured with ANTERA® CS (Miravex, Ireland) defines the skin degree of wrinkles with two parameters; overall size (a.u.) and depth ( $\mu\text{m}$ ).

## Results and Discussions

### Physicochemical characterization of LNP and SLE-LNP formulations

We first fabricated sets of lipid-based cosmetic formulations with varying compositions, as introduced in **Fig 1A**. Preparation method of the formulations was introduced the above. The appearance of lipid-based formulations with or without solid lipid enhancers(SLE) was observed using cryo-TEM. LNP, which prepared without any SLEs such as ceramide and fatty acids, shows uniform shade throughout the droplet, similar to the morphology of typical nanoemulsions (**Fig. 1B (left)**). However, LNP-C, which was added ceramide, exhibits dark band encircling the periphery of the nano-sized droplets. In addition, we could observe much more significant band in LNP-CF, which added SLE such as ceramide and fatty acids. This might be to the layer-by-layer structure from the lipid bilayer, as confirmed by SAXS data shown in **Fig 1C**. In the SAS pattern of LNP, there was no characteristic signals. While weak inflection peaks appear for LNP-C at  $q = 0.046, 0.07$ , and  $0.093 \text{ \AA}^{-1}$ , indicating the formation of lamellar structure based on the Bragg's law. In addition, LNP-CF with additional fatty acids show strong characteristic peaks  $q = 0.046, 0.07, 0.093, 0.115$ , and  $0.138 \text{ \AA}^{-1}$ , meaning lamellar structure with  $q$  value ratios of 2:3:4:5:6. This shows that the incorporation of fatty acids into LNPs might make structural packing state of LNPs increasing, contribute to colloidal stability. To check this point, we monitor the time-dependent change of particle size distribution over extended periods of time. As a result, we confirmed nonsignificant change in the mean diameter and the corresponding coefficient variation (CV) value for LNP-C and LNP-CF. While LNP significantly increased from  $63 \pm 3 \text{ nm}$  to  $315 \pm 22 \text{ nm}$  during 28 days incubation (**Fig 1D**). Although data was not shown in this article, we find that the zeta potential of SLE incorporated LNPs 28 days after incubation are  $\zeta = -31.0 \pm 0.9 \text{ mV}$  and  $\zeta = -45.9 \pm 1.1 \text{ mV}$  for LNP-C and LNP-CF, respectively. While the value of LNP is  $\zeta = -15.9 \pm 2.2 \text{ mV}$ , it was potentially unstable in the point of thermodynamics. Thus, these physicochemical results mean that solid lipid enhancers (SLE) such as ceramide and fatty acids contribute to stronger electrostatic repulsion between the neighboring LNPs, offering long-term colloidal stability of the formulation without aggregation or flocculation.

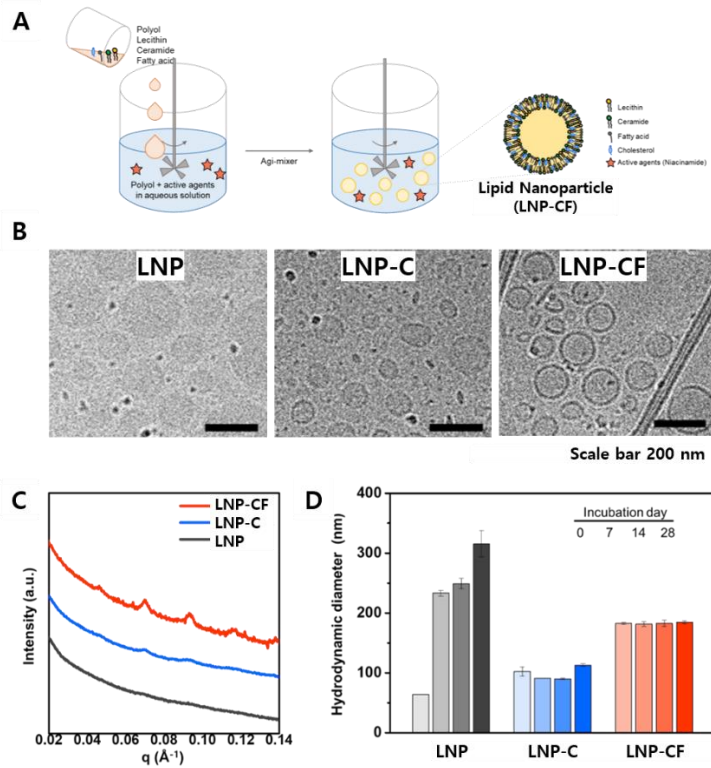


**Fig. 1** (A) Schematic image the preparation of LNP series. (B) Sets of TEM of the resulting LNP (left), LNP-C (center), and LNP-CF (right). Scale bars represent 200 nm. (C) SAXS patterns of the resulting LNP, LNP-C and LNP-CF. (D) Plot showing the hydrodynamic diameter of the resulting LNP series with respect to incubation time at room temperature.

### In vitro skin penetration study

To investigate the effect of SLE in skin penetration, we incorporate green fluorescent dye (FITC) in the DPG solution prior to preparation of sets of LNPs. The depth of skin penetration in each LNPs on 3D skin tissues was monitored using confocal laser scanning microscopy (CLSM) (**Fig. 2A**). We observe FITC signal only on the surface of the *stratum corneum* (SC) for LNP even after 4 h of treatment while deeper diffusion of FITC was shown for both LNP-C and LNP-CF. Then, to determine the effect of SLE on LNP formulations in the dermal delivery, we perform *in vitro* skin penetration study using Franz diffusion cell. In the Franz diffusion cell test, the amount of niacinamide permeated through the artificial synthetic membrane was monitored 2, 4, 8, and 24 h after application of the formulations. We confirmed that LNP-CF shows significantly higher penetration effect than LNP and LNP-C (**Fig. 2B**).

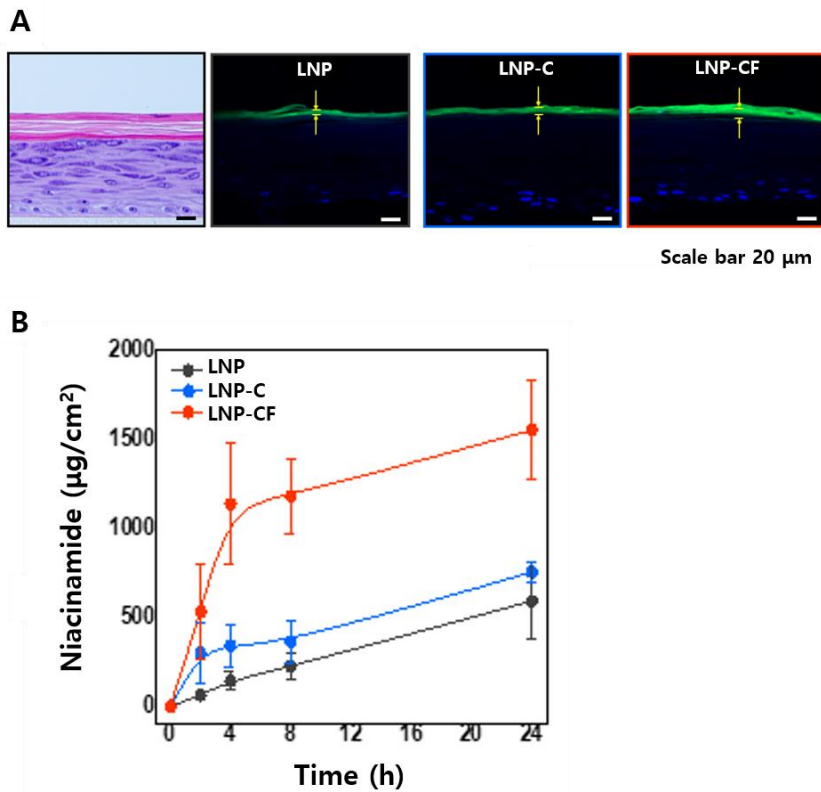


**Fig. 2** (A) Cross-sectional confocal laser scanning micrographs (CLSM) shows the penetration depth in 3D skin each treated with LNP, LNP-C, and LNP-CF, respectively. Nucleus is stained with DAPI (blue) for visualization. Scale bars represent 20  $\mu\text{m}$ . (B) *in vitro* niacinamide diffusion profile across artificial synthetic membrane.

#### *In vitro* skin brightening efficacy study

We investigate the advantage points of SLE-LNP including niacinamide with improved dermal delivery in skin depigmentation efficacy. Visual comparison on the histological cross-sections of the 3D skin with Fontana-Masson staining reveals that LNP-CF mostly effectively decreases melanin pigmentation in the reconstructed human pigmented epidermis by inhibiting the melanin transfer from the basal layer to the skin surface (Fig. 3A). In a different test, skin depigmentation efficacy was also evaluated using analogous lipid-based formulations containing arbutin. As a result, the efficacy of depigmentation on treating 8 days with LNP-CF was dramatically higher than LNP and LNP-C (Fig. 3B). The relative extent of depigmentation on the treated 3D skin were analyzed by acquiring the change of L-values after 8 days of treatment using a spectrophotometer. The values were  $8.4 \pm 0.8$ ,  $12.3$

$\pm 0.3$ ,  $12.5 \pm 0.5$ , and  $13.2 \pm 0.8$  for the control (PBS), LNP, LNP-C, and LNP-CF, respectively (**Fig. 3C**). It was demonstrated that all LNPs containing arbutin show depigmentation effects compared to the negative control (PBS). Of the LNPs, LNP-CF exhibits substantial brightening effect. This means that SLE improves the dermal delivery of active ingredients. Thus, the following *in vivo* skin efficacy test, we will primarily focus on comparing the efficacy of LNP without any SLE and the LNP-CF with ceramide and fatty acids.

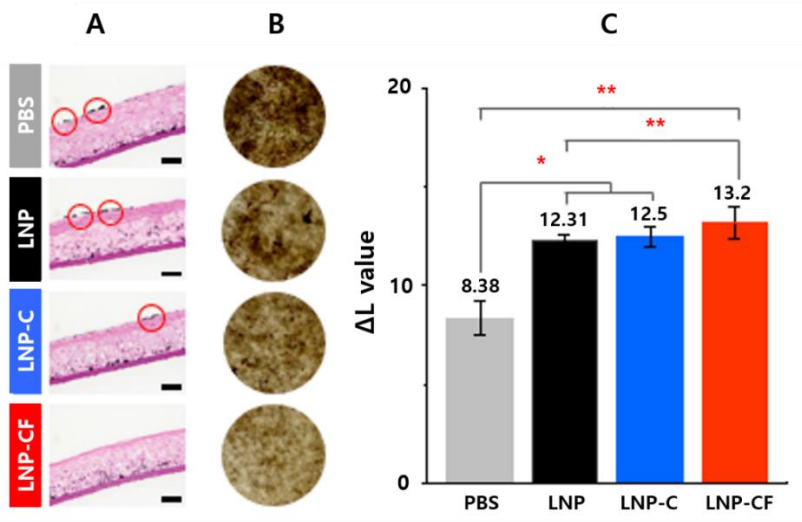


**Fig. 3** (A) Melanin pigmentation inhibition tests of cosmetic formulations (PBS, LNP, LNP-C, and LNP-CF) including niacinamide through 3D skin with Fontana-Masson staining. The red circles indicate the melanin transferred from basal layer to the skin surface. Scale bars represent  $50 \mu\text{m}$ . (B) Optical micrographs on 3D skin after exposure to cosmetic formulations (PBS, LNP, LNP-C, and LNP-CF) including arbutin for 8 days. (C) A plot showing the change of L-values for the 3D skin upon 8 days treatment with each cosmetic formulation including arbutin

### *In vivo* skin penetration study

To confirm the human skin permeation efficacy of LNP-CF, *in vivo* skin penetration study using confocal Raman spectroscopy was performed. To investigate the formulation permeation across the SC, the measurement was conducted at three different time points for each formulation. The penetration depth immediately after application (20 min) is  $18 \mu\text{m}$  and  $24 \mu\text{m}$  for LNP and LNP-CF, respectively. It means that LNP-CF more deeply and rapidly

permeates across SC than LNP. Moreover, it remains deep within SC even after absorption (60 min), as evidenced by the consistent penetration depth of 24  $\mu\text{m}$  for LNP-CF, unlike LNP which decreased to 16  $\mu\text{m}$ . In addition, the relative contents of formulation absorbed into the skin, estimated by determining the area reduction from immediately after application (20 min) to after absorption (60 min), corresponds to 21.4% and 25.5% for LNP and LNP-CF, respectively. This reveal that LNP-CF shows deeper penetration depth and faster permeation rate than LNP. Therefore, SLE would be helpful to improve skin penetration of cosmetic formulations.

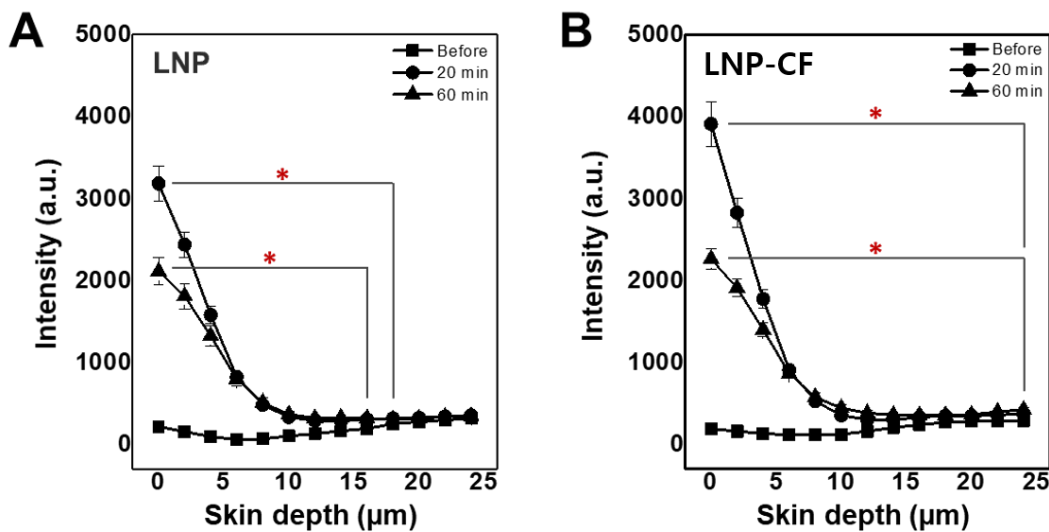


**Fig. 4** (A) Mean penetration content values of each formulation and their standard deviations obtained pre- and post-application at different time intervals (0, 20, 60 min) plotted against the skin depths of: (A) LNP and (B) LNP-CF.

#### *In vivo* skin brightening study

To compare *in vivo* skin brightening efficacy of LNP and LNP-CF containing niacinamide, 22 subjects who have hyperpigmentation sites were selected. The images of the subjects' cheek area as well as the skin melanin index were obtained before and after 2 and 4 weeks of usage, as shown in **Fig 5**. From the results, both LNP and LNP-CF containing niacinamide improve skin brightening. While LNP-CF exhibits statistically significant reduction in melanin index compared to LNP, resulting in the enhancement effect of skin efficacy.

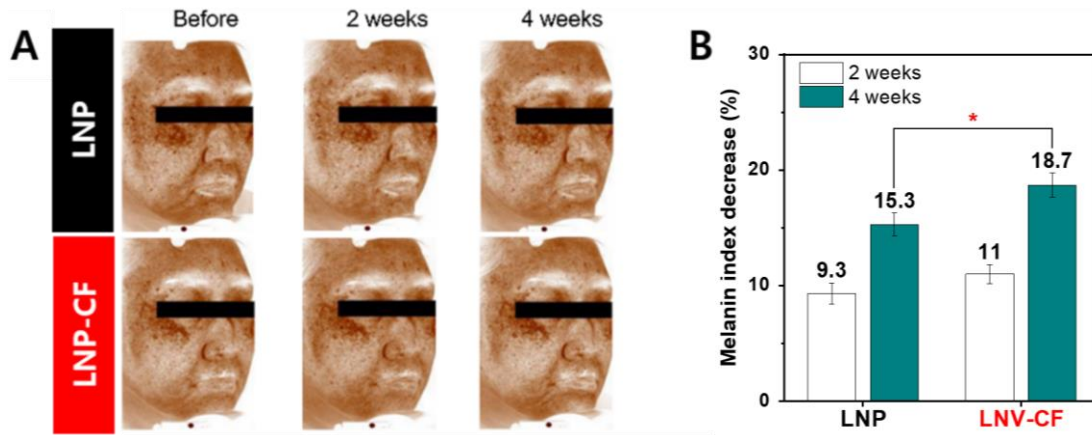


**Fig. 5** (A) Representative images of the subject's cheek area before and after 4 weeks of treatment with either LNP (top) or LNP-CF (bottom) containing niacinamide. (B) Plot showing the melanin index decrease (%) after 2 and 4 weeks of using either LNP or LNP-CF. Bars in both plots represent average and their standard deviation ( $n=22$ ). Statistical analysis was performed using *Paired t-test* and the *Mann Whitney U test*,  $*p < 0.05$ .

#### ***In vivo* skin wrinkle study**

Analogous to *in vivo* skin brightening efficacy test, 20 subjects with wrinkles around their eyes and a global photodamage score of 3 or more were selected to *in vivo* test the skin wrinkle improvement efficacy of LNP and LNP-CF containing adenosine. Images of the subjects' wrinkles around the eye area were obtained before and after 2 and 4 weeks of usage as shown in **Fig. 6A**. As a result, both LNP and LNP-CF containing adenosine shows good efficacy in the wrinkle reduction after 2 and 4 weeks of usage compared to before use. More importantly, LNP-CF exhibited statistically significant reduction in wrinkle parameters compared to control group (LNP), also indicating to a better skin efficacy enhancement effect. Thus, this clearly demonstrates that SLE such as ceramide and fatty acids mediates the delivery across the skin barrier layer.

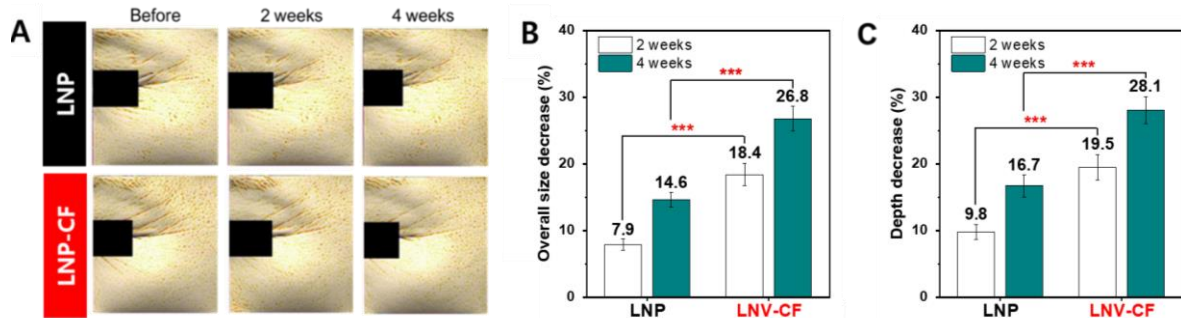


**Fig. 6** (A) Representative images of the subject's cheek area before and after 4 weeks of treatment with either LNP (top) or LNP-CF (bottom) containing adenosine. (B) Plot showing the overall size decrease (%) after 2 and 4 weeks of using either LNP or LNP-CF. (C) Plot showing the depth decrease (%) after 2 and 4 weeks of using either LNP or LNP-CF. Bars in both plots represent average and their standard deviation ( $n=20$ ). Statistical analysis was performed using *Paired t-test* and the *Mann Whitney U test*, \*\*\* $p < 0.001$ .

### Conclusion.

In conclusion, we introduced a novel approach in skin penetration of cosmetic formulation. Skin lipid enhancers (SLE), ceramide and fatty acids, are both incorporated in lipid nanoparticles (LNP) to mediate the delivery of active ingredients into the skin barrier layer. The introduction of SLE was shown to result in LNP with a lamellar structure and exhibit improved colloidal stability. Unlike previous skin enhancers such as chemical or physical enhancers, SLE are compatible with skin. Thus, it could enhance skin efficacy without skin damage. As a result of various *in vitro* and *in vivo* studies, we demonstrated SLE has much efficient in the skin delivery and efficacy. We anticipate that the ceramide and fatty acids incorporated LNPs presented in this work would be helpful to resolve the current issue associated with effectively delivering active ingredients across the skin barrier layer without skin damage.

### Acknowledgments.

This work was supported by the grant of the Korea Health Technology R&D Project through the Korea Health Industry Development Institute (KHIDI), funded by the Ministry of Health & Welfare, Republic of Korea (No. HP20C0006).

## **Conflict of Interest Statement.**

There are no conflicts to declare.

## **References.**

1. Akiyama M, Sawamura D, Shimizu H (2003) The clinical spectrum of nonbullous congenital ichthyosiform erythroderma and lamellar ichthyosis. *Clin Exp Dermatol* 28:235–240.
2. Cortés H, Magaña JJ, Reyes-Hernández OD, et al (2019) Non-invasive analysis of skin mechanical properties in patients with lamellar ichthyosis. *Ski Res Technol* 25:375–381.
3. Deepak RNVK, Sankararamakrishnan R (2016) Unconventional N-H...N Hydrogen Bonds Involving Proline Backbone Nitrogen in Protein Structures. *Biophys J* 110:1967–1979.
  
1. Marie-Alexandrine B, Stéphanie B, Jocelyne P, Yves C (2012) Penetration of drugs through skin, a complex rate-controlling membrane. *Current Opinion in Colloid & Interface Science* 17: 156-165.
2. Thomas S, Stefan L, Stefan S, Bodo D, Bruno D, Andreas L, Reinhard HHN (2019) The long periodicity phase (LPP) controversy part I: The influence of a natural-like ratio of the CER[EOS] analogue [EOS]-br in a CER[NP]/[AP] based stratum corneum modelling system: A neutron diffraction study. *Biochimica et Biophysica Acta (BBA) – Biomembranes* 1861(1): 306-315.
3. Gonneke SKP, A. Marjolein Engelsma-van Pelt, Henk KK, Joke AB (1999) Electron Diffraction Provides New Information on Human Stratum Corneum Lipid Organization Studied in Relation to Depth and Temperature. *J. Invest. Dermatol* 113: 403-409.
  
4. Julia C, Gert SG, Michelle J, Joke AB (2008) Lipid organization in human and porcine stratum corneum differs widely, while lipid mixtures with porcine ceramides model human stratum corneum lipid organization very closely. *Biochimica et Biophysica*

- Acta (BBA) – Biomembranes 1778(6): 1472-1482.
5. Ushera JR, Epand RM, Papahadjopoulos D (1978) The effect of free fatty acids on the thermotropic phase transition of dimyristoyl glycerophosphocholine. Chemistry and Physics of Lipids 22(3): 245-253.
  6. Golden GM, McKie JE, Potts RO (1987) Role of stratum corneum lipid fluidity in transdermal drug flux. Journal of Pharmaceutical Sciences 76(1): 25-28.
  7. Yoshikazu T, Yumiko Y, Shoji F, Kohji M, Kenji T, Hidehito Y, Syuichi K, Masao S (1998) Skin Penetration Enhancing Action of cis-Unsaturated Fatty Acids with  $\omega$ -9, and  $\omega$ -12-Chain Lengths. Biol. Pharm. Bull, 21(5): 484–491.
  8. Heather AEB (2005) Transdermal drug delivery: penetration enhancement techniques. Current Drug Delivery 2(1): 23-33